LARGE SCALE EXPERIMENTS ON BEACH EVOLUTION INDUCED BY BICHROMATIC WAVE GROUPS WITH VARYING GROUP PERIOD

Jose M Alsina[1], Ivan Caceres[2], Joep van der Zanden[3], Jan S. Ribberink[3] and Tom E. Baldock[4]

New large scale experimental data have been presented showing the wave group influence on beach morphodynamics at the surf and swash zones. Bichromatic wave conditions were generated varying the modulation bandwidth but keeping the wave energetic content constant within the experimentation limits. The wave group influence in the surf zone is observed in the form of the cross-shore location of the breaker bar respect to the initial still water level (SWL) location, which has been shown to increase as increases the wave group period. This influence is explained in terms of differences on the surf zone width induced by the varying wave group periods. In the swash zone, time dependent bed level elevation measurements were done using a newly developed conductivity technique, the CCM^+ system. Bed level time variations at the swash zone have shown to be composed of a long scale trend and bed level oscillations of shorter frequencies related to the wave group forcing. A good spectral correlation has been found between the water surface elevation and bed level variation at the wave group period for every bichromatic component indicating an important influence of wave groups on the swash zone morphodynamics.

Keywords: wave groups; beach morphology; bed level changes; swash zone; breaker bar location

INTRODUCTION

Wave grouping and associated bound long waves have been studied to be important for coastal zone sediment transport for many years (Butt and Russell, 2000; O'Hare and Huntley, 1994). It is currently assumed that most of the beach evolution and sediment transport is induced by short-scale wind and swell waves, although the morphological changes are based on sediment transport gradients that can vary over long-wave time scales (Baldock et al., 2011).

The convergences in wave energy density are inherent to the wave groups influencing the shoaling and wave breaking process in the surf zone. In addition, wave groups introduce further unsteadiness and intermittency into the short-wave processes that force sediment transport, i.e. wave-induced currents and turbulence. More importantly, the hydrodynamics in the inner surf and swash zones is largely affected by infragravity frequencies, particularly when dissipation influences the sea swell wave energy range more than the infragravity energy range. Dissipation of steeper waves at sea swell frequencies occurs mostly due to breaking in shallow water with energy transfer to gently sloping infragravity waves, for which breaking is less likely to occur.

The influence of wave groups and the associated bound long wave in sediment transport and beach morphology is complex but in general the bound wave is expected to give a seaward contribution to the transport, reducing shoreward transport outside the breakpoint. The presence of standing or partially standing waves inside the surf zone has been reported to be important in sediment transport and for longshore bar formation (O'Hare and Huntley, 1994). Close to the shoreline, infragravity swash motions can provide the main mechanism for sediment transport on low-sloping, dissipative beaches (Butt and Russell, 2000), and therefore, predicting their occurrence and magnitude is a critical component of coastal change models. Baldock et al. (2011) showed experimental data comparing variations in beach profile evolution between monochromatic waves, monochromatic conditions perturbed with free long waves and bichromatic wave groups with the same mean energy flux demonstrating that free long waves influence surf zone morphodynamics promoting in general increased onshore sediment fluxes compared to monochromatic conditions. In contrast, wave groups, which can generate both forced and free long waves, generally reduce onshore transport compared to monochromatic conditions.

The present work aims to isolate the influence of the wave group period in the sediment transport and beach profile evolution. Different bichromatic wave conditions were generated varying the wave group period but keeping the same energetic content. Differences in beach evolution will be presented in terms of the grouping period.

[1] Department of Civil and Environmental Engineering, Imperial College London, South Kensington Campus, SW7 2AZ, UK.
[2] Laboratori d'Enginyeria Marítima, Universitat Politècnica de Catalunya, C. Jordi Girona, 1-3 08034 Barcelona, Spain.
[3] Marine and Fluvial Systems group, University of Twente, Drienerlolaan 5, 7522 NB Enschede, The Netherlands.
[4] School of Civil Engineering, University of Queensland, St Lucia, QLD 4072, Brisbane, Australia.

EXPERIMENTAL SETUP

The present work was developed in the framework of the HYDRALAB IV access project: Coupled High Frequency Measurement of Swash Sediment Transport and Morphodynamics (CoSSedM). The experiments were carried out in the large scale wave flume CIEM at *Universitat Politecnica de Catalunya* (UPC), Barcelona. This is a wave flume 100 m long, 3 m wide, and 4.5 m deep (Figure 1). The working water depth was at around 2.5 m over the horizontal flume section and was varied slightly depending on the wave test. A beach was installed made of commercial well-sorted sand (d_{50} = 0.25 mm, d_{10} = 0.154 mm and d_{90} = 0.372 mm) with an overall mean beach gradient of approximately 1:15. The measured sediment settling velocity is of 0.034 m/s. The beach commenced 33.3 m from the wavemaker with the toe of the beach at an elevation of around −2.5 m relative to the SWL and approximately 42 m seaward of the SWL cross-shore location.

The range of instrumentation utilized in the CoSSedM experiments (Figure 1) included wire wave gauges (WG) along the length of the flume, Pore Pressure Transducers (PPT) in the surf zone and acoustic wave gauges (AWG) in the inner surf and swash zone. A series of Acoustic Doppler Velocimeters (ADV) and Optical Backscatter Sensors (OBS) were also distributed in the surf and swash zones. Instruments measuring water surface elevation (WG, AWG and PPT) were calibrated during changes of water level in the flume (approximately once every two days). The beach evolution along the center-line of the wave flume was measured with a mechanical wheeled bed profiler that measures both the sub-aerial and submerged beach elevation.

A new Conductivity Concentration Meter (CCM$^+$) system (van der Zanden et al., 2013) was installed in the wave flume within the swash zone. The new CCM$^+$ system consisted of a total of four sensor probes that can move in the vertical direction and that are part of two large tanks, plus a control box and operating system. The tanks were buried in the beach so the probes moved up and down from underneath to measure water conductivity at a known vertical elevation with minimum flow disturbance. The CCM system is able to simultaneously measure the continuous bed-level as well as (sheet-flow) sediment concentrations and particle velocities. The tanks and probes were located at two different locations within the swash area (Figure 1), x = 75.81 m (CCM probes 1/2 and 3, tank 1) and 77.8 m (CCM probe 4, tank 2). Tank 1 location was observed to be located at the lower swash sub-zone while tank 2 was observed to be in a mid-swash location or upper swash location depending on the wave conditions. The swash zone sub-areas were identified according to submergence ratios (Aagaard and Hughes, 2006).
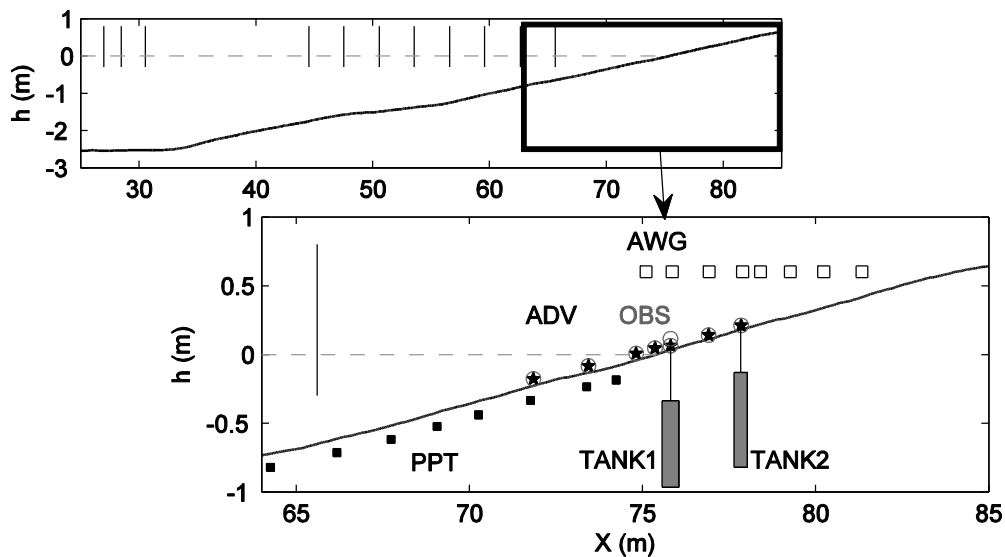

Figure 1. Wave flume configuration with measured initial bathymetry. General view with resistive wave gauge positions, and amplification of the beach-face area subject of interest with instrument locations. Solid squares are PPTs, open squares are AWGs, open circles correspond to OBSs and stars symbols mean ADVs.

Different tank cross-shore locations relative to the swash zone limits were obtained for a selection of wave conditions by slightly modifying the working water depth. This is the reason why we have

repeated wave conditions with different water depths. This choice was preferred over burying the tanks at a different location for each test (highly time consuming). The CCM tanks capabilities to measure at the swash zone and technical details have been investigated, preliminary results have been presented in van der Zanden et al. (2013) with a more detailed description expected to be released in the near future.

The experimental program was divided into two test series (erosive and accretive), and within each test series a number of different wave cases were generated. The measured wave conditions are specified in Table 1. For the present paper, only the erosive conditions are considered. The different bichromatic wave conditions were designed to have a similar flux of energy and spectral energy content. The dimensionless sediment fall parameter ($\Omega = H_0/w_sT$) and surf similarity parameter, or Iribarren number ($\xi = \dfrac{\tan\beta}{\sqrt{H_0/L_0}}$ where H_0 and L_0 are the wave height and wave length at the offshore boundary and $tan\beta$ is the beach slope), have been also included in Table 1. The dimensionless sediment fall parameter is generally used to classify beach states (Wright and Short, 1984), and as a descriptor of beach profile evolution and on/off-shore sediment transport dominance (Dean, 1973). The dimensionless sediment fall parameters are within a narrow range of 2.8-3.5 for the erosive conditions, predicting a similar erosive behavior for the different test series.

Table 1 – Performed erosive wave conditions with wave height obtained from spectral moment at sensor located closer to the wave paddle (x = 7.72 m shoreward from the toe of the wavemaker). * BE4 data not shown because the resistive wave gauges close to the wave paddle failed for this condition.

Wave Case	Component 1		Component 2		T_{gr} (s)	Ω	ξ	d (m)
	H_1 (m)	f_1 (Hz)	H_2 (m)	f_2 (Hz)				
BE1	0.29	0.303	0.26	0.237	15.15	3.08	0.429	2.53
BE1_2	0.30	0.303	0.26	0.237	15.15	3.12	0.427	2.48
BE2	0.26	0.30	0.24	0.239	16.38	2.80	0.448	2.50
BE3	0.31	0.295	0.31	0.246	20.48	3.53	0.402	2.50
BE4[**]		0.288		0.251	27.31			2.50
BE4_2	0.28	0.288	0.30	0.251	27.31	3.27	0.417	2.46

A typical test series (BE1, BE2, and so on) started from the same plane 1:15 sloping bed manually reshaped beach profile and a series of 8 (7 for BE1 case) hydrodynamic run. Each run consisted of approximately 30 minutes of wave action (240 minutes in total, 210 BE1 case). The beach profile is measured after each run, having a total of 9 measured beach profiles per test (8 for BE1 case).

RESULTS AND DISCUSSIONS

As explained in the Introduction, the main aims of the present experiments were to investigate the role of wave groups and associated bound long waves in the hydrodynamics, sediment transport and beach evolution (i.e. morphodynamics). Two different effects of varying wave groups on beach morphodynamics have been identified: i. a variation of the cross-shore location of the breaker bar, and ii. varying bed level changes at the wave group time scale in the inner surf and swash zones. Both mechanisms will be explained next.

Group period influence in the overall beach profile evolution

The four erosive generated bichromatic conditions aimed to have the same energetic content and flux of energy. They were designed to have the same primary wave variance-based bichromatic wave height H_{bi} of 0.4 m and a primary short wave group frequency $f_p = (f_1+f_2)/2 = 0.21$Hz. In reality, the measured water surface elevation showed slight differences from the designed ones due mainly to some discrepancies in the empirical wave paddle transfer function for different mean water depths and periods. As a result the measured H_{bi} showed slight differences among the different tests. This is illustrated by the differences in the computed dimensionless fall velocity (Ω) in Table 1 which varies slightly between different erosive tests.

The mean initial and final measured beach profiles for each wave condition are illustrated in Figure 2. The four tested bichromatic wave conditions resulted in beach erosion, shoreline retreat and the development of a bar at around the wave breaking location (breaker bar). Although values for the dimensionless fall velocity Ω are similar for the four presented cases (Table 1), considerable changes, in the equilibrium profiles measured were observed. In particular, the location of the breaker bar shows

a direct relationship with the wave group period, with an increasing distance to the initial SWL location ($x = 0$) with increasing wave group period.
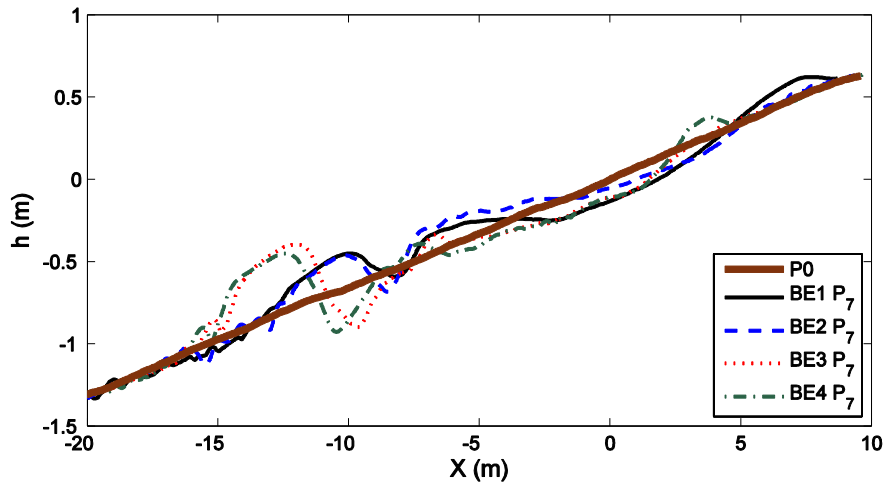

Figure 2. Mean initial beach profile (P0) and final (equilibrium) beach profile measurement (P7) for the four bichromatic erosive conditions.

The bar cross-shore locations and elevation have been computed from the measured beach profiles as the peak bed elevation in the breaker area (minimum profile elevation in absolute value). Figure 3 displays the cross-shore bar location time evolution for the different test cases. The cross-shore bar location is referenced with respect to the initial shoreline location giving an absolute value. A rapid cross-shore bar migration is observed at the beginning of the experiments for most of the test conditions (BE1, BE3 and BE4) followed by a quasi-equilibrium situation in which the bar migration almost stops.
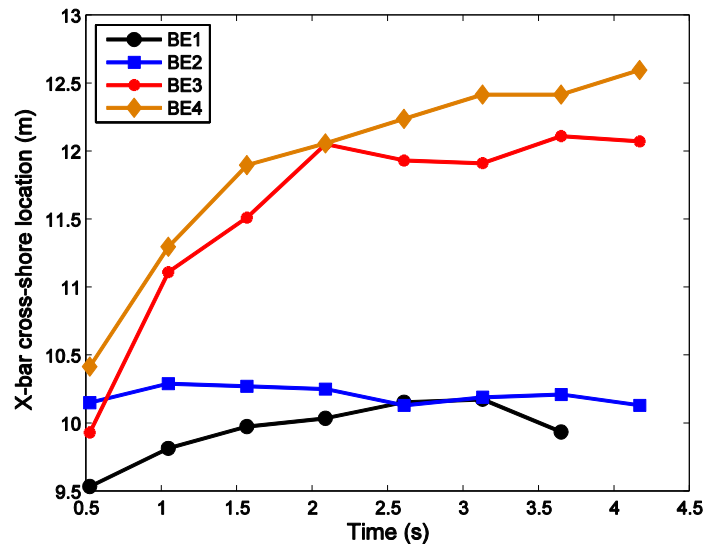

Figure 3 – Time series (in experimentation time) of cross-shore bar location for the different test cases.

It is also very interesting that the time necessary for the bar migration to become almost constant, indicating a quasi-equilibrium condition, increases with increasing wave group periods. A larger variability on the bar cross-shore location is observed for cases BE3 and BE4 respect to BE1 and BE2. For BE1 and BE2, the breaker bar seems to have reached an equilibrium position after the initial test case. BE1 and BE2 cases (0.066 and 0.060 Hz of group frequency respectively) show a similar cross-

shore bar location during part of the experimentation time. This is partly due to the methodology to compute the bar location and the bed variability. Another aspect to consider here is that the dimensionless sediment fall velocity parameter (Ω, Table 1) is smaller for case BE2 than BE1 and therefore BE2 should have a trend that is less erosive than BE1 (i.e. according to Ω values, BE2 would promote a bar located more shoreward than the bar location for case BE1).

The wave group influence on the cross-shore evolution of the breaker bar can be explained in terms of the mean wave breaking cross-shore location. Mean breaking location has been computed from the experimental data as the location where approximately half the offshore incident wave energy would be dissipated, i.e. $(H_{rms}/H_{rms0})^2=0.5$. This may be written as $H_b = H_{rms0}/\sqrt{2}$. The cross-shore location is found by interpolating the H_b value from the measured cross-shore wave height distribution. Figure 4 shows the computed mean cross-shore breaking location and cross-shore bar location for the different wave conditions as a function of the wave group periods.
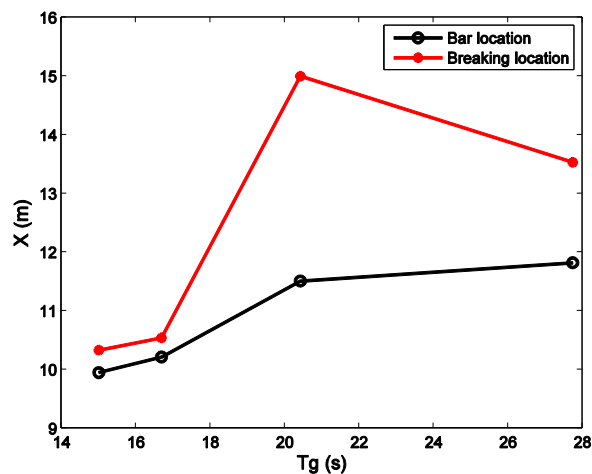

Figure 4. Cross-shore bar and wave breaking locations as a function of wave group period.

The data presented in Figure 4 show an offshore shift of the mean wave breaking location and cross-shore bar location as the wave group period increases. Bar migration has been associated to wave breaking intensity (Dally, 1987; Roelvink and Stive, 1989; Thornton et al., 1996) and to the feedback between breaking induced undertow and the sand bar location (Gallagher et al., 1998). The role of long waves in bar migration has also been discussed in the literature, particularly relating generation and migration to standing infragravity waves, with bars forming or moving towards the antinodes of standing infragravity waves (Bowen, 1980; Holman and Bowen, 1982). We have not found any evidence of this long wave mechanism in the present data. More details on this topic will be presented in a future publication.

Therefore, the wave group induced breaking location and its influence on the breaking induced flows and sediment transport is thought to explain the different bar evolution although velocities or sediment concentration in the surf zone were not directly measured in the present experiments. It is known that wave energy density focusing is inherent to wave groups propagation influencing the shoaling and wave breaking process (Holthuijsen and Herbers, 1986).

Apart of the wave group influence on the bar cross-shore location, the wave group has shown to modify the pattern of shoreline erosion and berm location as illustrated in figure 2. A more detailed plot of beach profile evolution at the inner surf and swash zone for the two extreme wave group periods (case BE1 and BE4, T_{gr} of 15.15 and 27.31 s respectively) is displayed in figure 5 to better illustrate the wave group influence in the beach profile evolution in this area. The shorter wave group condition (BE1) induced larger shoreline erosion and a wider berm located further onshore than the larger wave group case (BE4) that promoted less shoreline erosion although the erosion extend further in the inner surf zone (x ~-7m, BE4, compared to x~-4m, BE1). Increasing the wave group period seems to have an effect of shifting the active beach profile seaward.

This influence displayed in figure 5 cannot be extrapolated to all the cases since BE2 displayed a larger shoreline erosion than BE1, although located in a narrower area (less eroded volume), and BE2

and BE3 displayed a flatter berm (refers to figure 2 for more detail) than BE1 and BE4. Therefore, although an influence of wave groups in the shoreline morphodynamics is suggested, we could not find a measured parameter relating major characteristic of the beach profile evolution to the wave group periods for every case as it happened for the breaker bar cross-shore location.
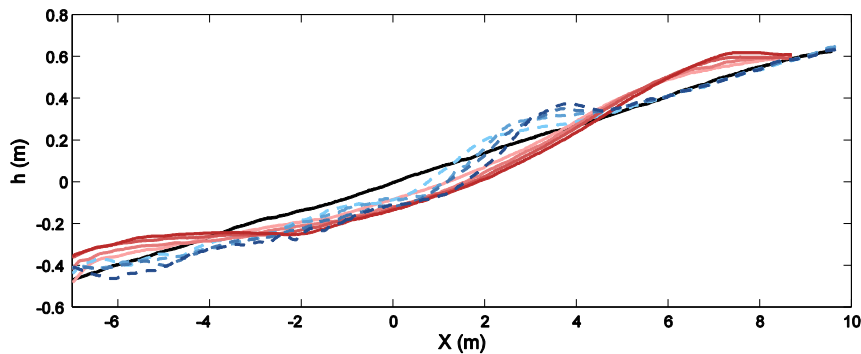

Figure 5. Detail of measured mean initial beach profile (black line) and beach profile evolution for cases BE1 (solid lines) and BE4 (dashed line). The color intensity indicates for each case how close the measured profile is of the final state being the final measured profile the darker color.

Group period influence in the time-dependent bed level evolution at the swash zone

In the present experiments, high frequency measurements of swash zone bed evolution were possible using conductivity probes, the CCM$^+$ system. Time-dependent but short wave averaged bed level measurements will be shown and the influence of wave group period illustrated next.

A detailed explanation of the new CCM$^+$ measuring technique and how sediment concentration and movable bed level are obtained can be found in van der Zanden et al. (2013). Conductivity probes are able to measure high concentration values very close to the bed level and of the order of the packed sediment in the stable bed. The new CCM$^+$ concentration tracking system consists of a feedback loop between concentrations and sensor vertical movement, enabling the sensor to move vertically to the direction of a given target concentration. This feedback and the simultaneous concentration and vertical elevation measurements allow bed level tracking and sediment concentrations relative to a moving bed level. The CCM$^+$ probes in quick tracking mode cannot follow instantaneous concentration changes (time scales smaller than short incident waves), but they are well able to follow gradual bed-level motions that occur on time scales > seconds.

Figure 6 displays time series of computed bed level using measured vertical elevation from CCM$^+$ (in quick tracking mode) using the initial vertical elevation as reference level (0 bed level). The test conditions correspond to BE1 and BE4, and the cross-shore locations relative to the initial SWL are $x = 0.56$-0.45 m, cases BE1 and BE4 (tank 1, Figure 6a), and $x = 2.59$-2.48 m for cases BE1 and BE4 respectively (tank 2, Figure 6b), shoreward of the initial SWL. The bed level is computed here as the short wave-averaged bed-level, which can be obtained by applying a low-pass Fourier filter on the positions of the conductivity probe. The Fourier transform-based filter was applied with a cut-off frequency of 0.1 Hz (for both cases BE1 and BE4). Therefore, we are focusing on bed level oscillations occurring at a time scale of the order of the wave group (the wave group period was 15.15 s for case BE1 and 27.7 for case BE4, table 1). Notice that bed level measurements during the two first tests of BE4 case are not available. This is because the hydrodynamic data of this case could not be recovered and therefore comparison with AWG data was not possible, but also because BE4 was the first measured case and we believe that the initial CCM conductivity setting was not appropriate but corrected after the second test.

Bed levels were also computed from the Acoustic Wave Gauge (AWG) signal and a mobile computation of the signal minimum values. A mobbing window of the order of the wave group period was used. This methodology provides a continuous bed level computation very similar to analyzing the acoustic wave gauge signal and identifying the elevation during periods of bed exposure, for which the measured signal is constant or equal to the sensor noise (Turner et al., 2008). Figure 6b illustrates the comparison of the obtained bed level computed using the CCM$^+$ probe, (tank 2) and the bed level estimated from the co-located AWG. The agreement is good given the instruments accuracy (order of mm). Notice that for tank 1, cross-shore location x = 0.56-0.45 m, comparison of computed bed level

between CCM[+] and AWG instruments were not always possible since the emergence periods for this location were often shorter than the selected threshold and the minimum values computation was not considered reliable either since we were not sure if the bed under the AWG sensor was submerged or emerged.

Bed elevations obtained from the wheeled bottom profiler at the wave flume center-line after tests are also illustrated in Figure 6a and b for tank 1 and 2 locations respectively. The agreement respect to the CCM and AWG measurements is relatively good for tank 2 but not as good for tank 1.
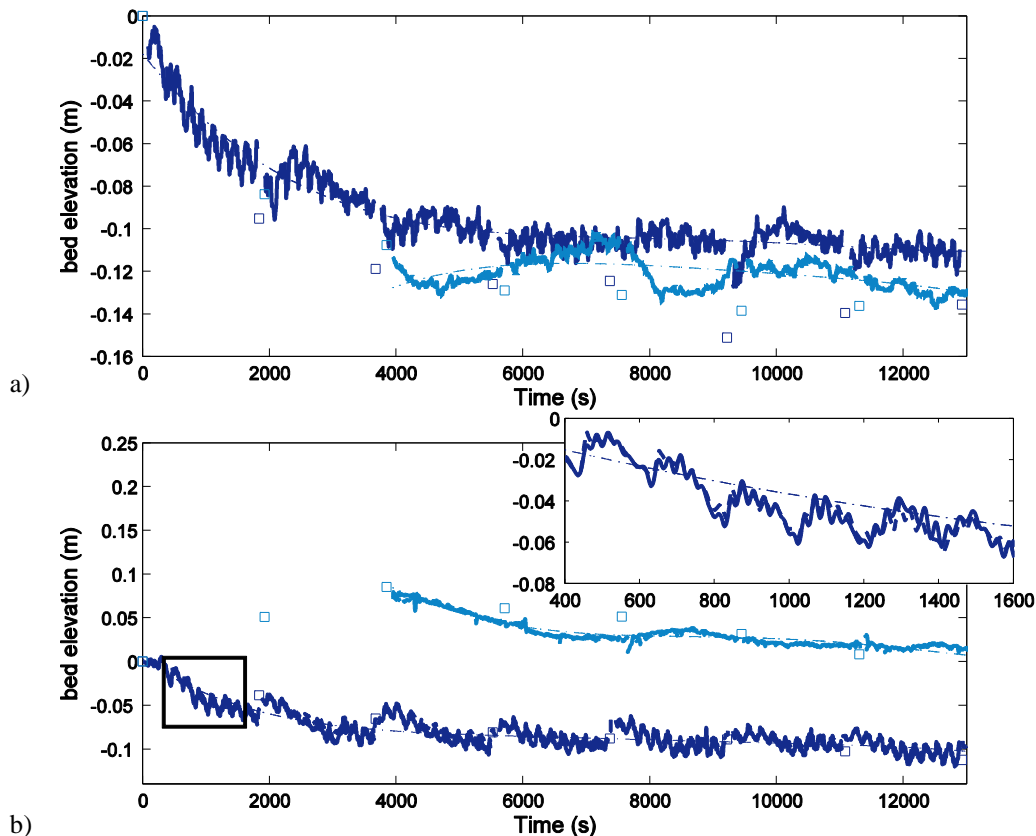

a)

b)

Figure 6. Time series of computed bed level from *CCM+* system (solid line), AWG (dotted line, plot a only) bottom profiler (squares), and trend line of CCM levels (dash-dotted line). Plot a: CCM tank 1 with cross-shore location x = 0.56 m (BE1) and 0.45 m (BE4) Plot b: CCM tank 2 with cross-shore location x = 2.59 m (BE1) and 2.48 m (BE4). Darker lines correspond to BE1 case while lighter lines correspond to case BE4

From Figure 6 it is observed that the time-dependent (low-pass filtered) computed bed level is composed by bed level change components at different time scales. A longer term (of the order of the experimentation time) trend is illustrated by the polynomial fit (dash-dotted line) which, similarly to the time evolution of the bar locations illustrated in Figure 3, shows a rapid bed evolution during the initial experimentation time (experimentation time from 0 to 4000 s) and a flatter trend at the end of the experimentation time consequent with the beach evolution reaching an equilibrium situation. The longer trend showed total erosion at the tank 1 location, in the lower swash zone, of the order of 11 and 13 cm for cases BE1 and BE4 respectively. On the other hand, tank 2 location (mid swash) showed an erosive behavior for test BE1 of 11 cm while BE4 exhibited an initial berm (accretion) that migrated shoreward afterwards displaying an erosive trend after a experimentation time of 4000 s (Figure 6b), resulting in a final net gain of 1 cm of bed level.

In addition, the plots of Figure 6 and in particular the inset of Figure 6a show that the bed oscillates around the long-term trend with erosive and accretive cycles of different time periods, identified as 15, 27, 32.7 and ~200s for BE1, corresponding to the wave group frequency, approximately two times the wave group frequency and the repetition frequency (f_r). It has been observed that the same wave group structure for case BE1 repeated every two groups (31 s) within a longer repetition cycle of every 13 groups (197s) approximately. For case BE4 the oscillations

correspond to 27.8 s. The characteristic periods can be identified by spectral analysis as illustrated in Figure 7. The bed level oscillations are more evident for the shorter wave group period (BE1), and amplitudes are higher for the CCM tank which is most shoreward.

The identified bed level oscillations are related to the generated wave group condition. The degree of correlation between the generated wave condition and bed level oscillations has been studied using spectral techniques. Power spectral density, cross-spectrum and spectral coherence (magnitude-squared coherence, MSC), have been computed for the computed bed level oscillation, de-trended using the polynomial fit shown in Figure 6, and the band-pass filtered water surface elevation at the location $x = 0.56$-0.45 m (tank 1). The applied filter is a Fourier based filter and the cut-off frequencies for the water surface elevations are 0.003 and 0.1 Hz, therefore only the components at the range of the de-trended bed level oscillations are considered. The selected location corresponds to the lower swash zone and therefore the computed bed level is also removed from the water surface elevation signal. Power spectral density (PSD) has been computed at this location for both signals and the relative values, scaled to the maximum value, are displayed in Figure 7.

Two different methodologies for computing the PSD, cross-spectrum and MSC have been considered, the first one use the whole bed level and water surface signal during the experimentation time and a second one separating the time series in the different tests, removing the first and last wave groups and averaging between tests. Both methodologies produced very similar results but the averaging between tests results in a slightly smoother plot which is the only methodology displayed here for clarity reasons. Figure 7 shows the PSD of bed-level measurements (CCM[+]) and water surface elevations at the position of tank 1, with the left and right plots corresponding to case BE1 and BE4, respectively. In the other hand, Figure 8 shows the obtained MSC values between the computed bed levels and the filtered water surface elevation.
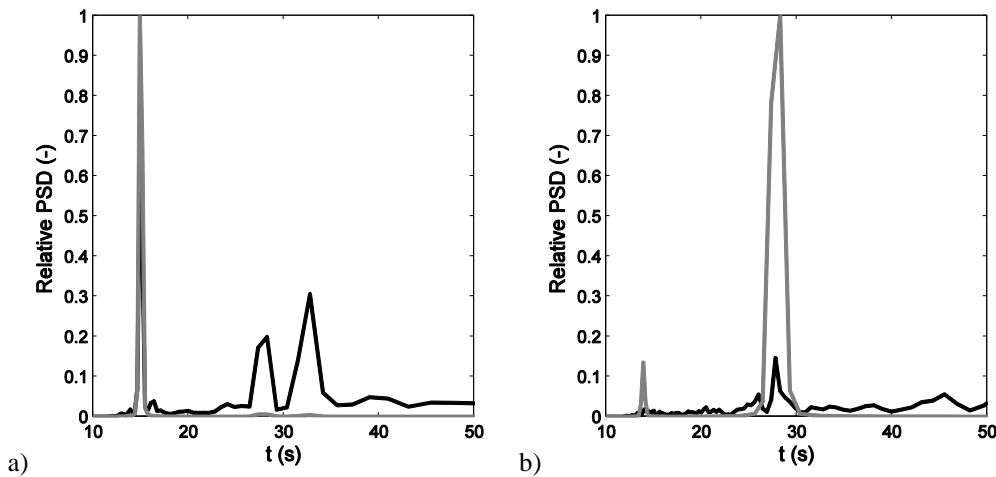

Figure 7. Computed relative power spectral density of the computed bed level using the CCM[+] technique (black lines) and the band-pass filtered water surface elevation (grey lines) at the location x = 0.56-0.45 m for case BE1 (a) and BE4 (b).

MSC is defined as the squared cross-spectral density between the two signals divided by the product of the spectral density of the signals, and it is a measure of the spectral correlation between the two signals. Its value ranges from 0, indicating no relation between the two signals, to 1 when a perfect relation exists. The computed MSC displayed in Figure 8 shows a close relation between the water surface elevation and the bed level changes at the wave group period for both cases, with high MSC values (0.9 and 0.6 for cases BE1 and BE4 respectively) at the wave group periods $T_{gr} = 15.16$ s (BE1) and 27.7 (BE4). Similarly, high coherence is found at other frequencies. For example, for case BE1 high MSC values are found at around of two times the wave group frequency (T = 28 and 34 s and MSC values of 0.65 and 0.75) identified with wave group repetition and at the repeated period $T_R \sim$ 190s (MSC 0.48) the later not shown in Figure 7 for clarity. On the other hand for case BE4 a relatively high MSC value is found at half the wave group frequency, MSC of 0.42 at T = 13.8 s.

Phase lags between the bed level and water surface oscillations for the periods providing highest MSC values have been obtained from the cross-spectral density computation. The obtained phase lags at the wave group frequency are of 150 and 140 degrees for cases BE1 and BE4 respectively (tank 1 location). The two signals are relatively close to 180 degrees out of phase, indicating minimum levels of bed level oscillation (erosion) close to the peaks of the water surface at the wave group frequency for both bichromatic cases.
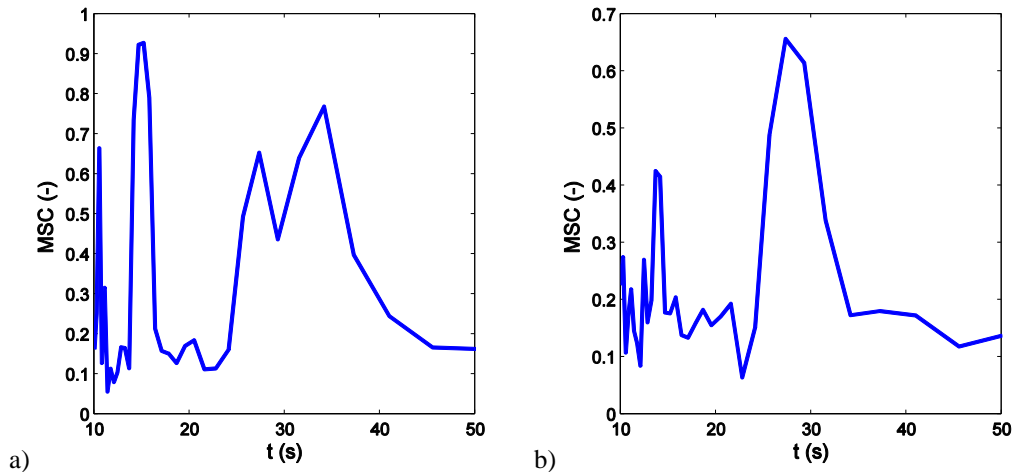

Figure 8. Computed magnitude-squared coherence (MSC) between the computed bed level using the CCM⁺ technique and the band-pass filtered water surface elevation at the location x = 0.56-0.45 m for case BE1 (a) and BE4 (b).

CONCLUSION

New large-scale experimental data have been presented on the influence of wave groups on the beach profile evolution and bed level changes in the swash zone. Bichromatic wave conditions were generated having a similar energetic content, i.e. similar total wave height and mean primary wave frequency ($f_{pm} = (f_1+f_2)/2$) but with varying wave group periods. Four different wave group periods have been tested, i.e. T_{gr} = 15.17, 16.67, 25 and 27.7 s. Small differences in energetic content between test cases are attributed to wave generation and the semi-empirical transfer function used for the wave paddle.

The different wave group periods have shown to have an important influence on the beach morphology: firstly in the surf zone through changes in the cross-shore location of the beaker bar, and secondly in the swash zone by affecting the shoreline erosion and berm formation pattern.

In the surf zone, the beach evolution measurement shows a direct influence of the wave groups on the cross-shore location of the breaker bar, with an increasing bar distance to the initial SWL as the wave group period increases. This wave group influence is explained in terms of the surf zone width, the length of the surf zone is shown to increase as the wave group period increases in a similar fashion as the bar location. The surf zone width is shown to have also an impact on the bar location variability during experimentation time. Longer wave groups (larger surf zone width) showed to promote a larger variability of the bar location during experimentation time needing longer time to reach a stable condition than shorter wave groups.

In the swash zone, another trend can be observed in shoreline retreat and the location of berm formation. The experimental data show that the berm at the swash zone tends to be generated further seaward with increasing wave group period and the shoreline retreat tends to increase inversely with increasing wave group period. This trend is not as clear as for the bar cross-shore location because of the difficulties defining a parameter reflecting this influence, and because of the small differences in energetic content between cases. For example, case BE2 showed a larger shoreline retreat than case BE1 although the extension where erosion occurs towards the bar location was smaller and therefore the erosion volume was smaller than BE1. Moreover case BE2 did not show a berm formation as clear as for cases BE1, BE3 or BE4 (Figure 2).

Conductivity measurements using a newly developed CCM$^+$ system allowed a continuous bed level elevation measurement at the wave group scale by low-pass filtering the measurement of the bed-water interface vertical elevation. Bed level elevations computed using the CCM probe match very well with the bed measurements obtained using acoustic sensors during emerged swash periods. The time-dependent bed level elevation showed a long time scale bed evolution trend and a smaller scale contribution well correlated to the wave groups. Spectral density analysis of the bed level changes at the low swash location showed a good correlation with the water surface elevation at the wave group frequency expressed in the computed magnitude-squared coherence.

ACKNOWLEDGMENTS

REFERENCES

Aagaard, T. and Hughes, M.G., 2006. Sediment suspension and turbulence in the swash zone of dissipative beaches. *Marine Geology*, 228(1-4): 117-135.

Baldock, T.E. et al., 2011. Large-scale experiments on beach profile evolution and surf and swash zone sediment transport induced by long waves, wave groups and random waves. *Coastal Engineering*, 58(2): 214-227.

Bowen, A.J., 1980. Simple models of nearshore sedimentation: Beach profiles and longshore bars. In: *S.B.M. Cann (Editor), The coastline of canada*, pp. 1-11.

Butt, T. and Russell, P.E., 2000. Hydrodynamics and cross-shore sediment transport in the swash-zone of natural beaches: A review. J*ournal of Coastal Research*, 16(2): 255-268.

Dally, W.R., 1987. Longshore bar formation, *Proceedings of Coastal Sediments'87*. Am. Soc. of civil Eng., New York, pp. 71-86.

Dean, R.G., 1973. Heuristic models of sand transport in the surf zone. Engineering Dynamics of the Coastal Zone: F*irst Australian Conference on Coastal Engineering*, Sydney, pp. 208–214.

Gallagher, E.L., Elgar, S. and Guza, R.T., 1998. Observations of sand bar evolution on a natural beach. *Journal of Geophysical Research*, 103(C2): 3203-15.

Holman, R.A. and Bowen, A.J., 1982. Bars, bumps and holes: Models for the generation of complex beach topography. *Journal of Geophysical Research*, 87: 457-468.

Holthuijsen, L.H. and Herbers, T.H.C., 1986. Statistics of breaking waves observed as whitecaps in the open sea. *Journal of Physical Oceanography*, 16(2): 290-297.

O'Hare, T.J. and Huntley, D.A., 1994. Bar formation due to wave groups and associated long waves. *Marine Geology*, 116(3–4): 313-325.

Roelvink, J.A. and Stive, M., J. F., 1989. Bar-generating cross-shore flow mechanisms on a beach. *Journal of Geophysical Research*, 94(C4): 4785-4800.

Thornton, E.B., Humiston, R.T. and Birkemeier, W.A., 1996. Bar/trough generation on a natural beach. *Journal of Geophysical Research*, 101(C5): 12097–12110.

van der Zanden, J., Alsina, J.M., Caceres, I., Buijsrogge, R.H. and Ribberink, J.S., 2013. New ccm technique for sheet flow measurements and its first application in swash zone experiments. *Proc. 6th International Short Course/Conference on Applied Coastal Research*, 4-7 June, Lisbon, Portugal.

Wright, L.D. and Short, A.D., 1984. Morphodynamic variability of surf zones and beaches: A synthesis. *Marine Geology*, 56(1-4): 93-118.